ACS APPLIED MATERIALS & INTERFACES

LETTER

www.acsami.org

Optical Nanosensor Platform Operating in Near-Physiological pH Range via Polymer-Brush-Mediated Plasmon Coupling

Ihor Tokarev, Iryna Tokareva, and Sergiy Minko*

Department of Chemistry and Biomolecular Science, Clarkson University, Potsdam, New York 13699, United States

ABSTRACT: The nanosensors' platform made of a stimuli-responsive polymer/noble metal nanoparticle composite thin film exploits the combination of the swelling−shrinking transition in a poly(*N*,*N*′-dimethylaminoethyl methacrylate) brush and the localized surface plasmon resonance in metal nanoparticles to enable the transduction of changes in the solution pH in the near-physiological range into a pronounced optical signal.

KEYWORDS: polymer brushes, enzymatic biosensors, stimuli-responsive materials, localized surface plasmon resonance, thin films

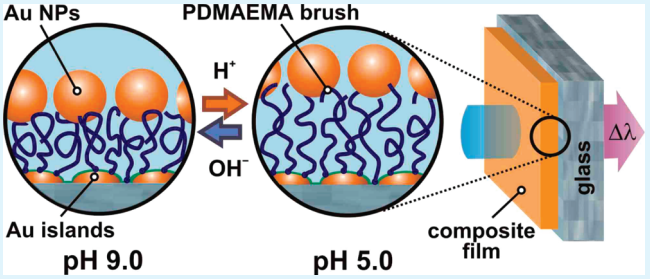

This letter describes a chemical/biochemical sensors' platform that exploits the combination of two distinct phenomena — (1) the swelling−shrinking transition in a stimuli-responsive polymer thin film and (2) the localized surface plasmon resonance (LSPR) in noble metal nanoparticles that reside in the film. This combination enabled the transduction of changes in the analyte concentration into an optical signal. Specifically in this work, we report on the sensor platform that is sensitive to changes in the solution's pH in the near-physiological range (between pH 5 and pH 9). This finding opens new opportunities for the development of sensors for biochemical/biomedical analytes.

The sensitivity of LSPR spectra to the particles' environment and the interparticle distance is attributed to evanescent waves localized on the metal surface. Because the evanescent field strength decays exponentially with the distance, the nanoparticles "sense" only their immediate environment. The interparticle interactions via the evanescent field are often referred to as plasmon coupling, which leads to strong modification of the LSPR spectra. The LSPR in metal nanoparticles have been broadly explored for analytics.[1−5] Recently, the LSPR phenomenon has been used in a combination with stimuli-responsive polymers for miniaturized sensors. Noble metal nanoparticles associated with responsive polymeric materials[6,7] were used to probe swelling−shrinking transitions in polymer chains triggered by a specific environmental stimulus, such as temperature, pH, ionic strength, or solvent quality. The volume phase transition in the polymer caused changes in the refractive index in the vicinity of the particle surface and induced changes in the characteristic interparticle distance. Examples include polymer brushes[8] tethered to the surface of an optically transparent substrate[9−15] or colloidal carriers,[16−20] polymer/nanoparticle hybrid microgels,[21] multilayers assembled using metal nanoparticles as building blocks,[22,23] hydrogel/nanoparticle hybrid films[24,25] and membranes,[26] and hybrid nanotubes composed of a block copolymer and metal nanoparticles.[27]

In our previous studies, we explored the sensing platform when a responsive polymer brush was tethered to the surface of a glass substrate with a deposited monolayer of nanoislands (gold or silver) and served as a matrix for the incorporation of colloidal nanoparticles of the same metal.[28,29] The brush thickness was chosen so that the nanoparticles and nanoislands experienced pronounced plasmon coupling and, at the same time, polymer chains undergoing the swelling−shrinking transition actuated the nanoparticles to ensure considerable variations in the characteristic spacing between the brush-entrapped nanoparticles and the immobile nanoislands. The system composed of gold nanoparticles and nanoislands coupled with an ultrathin brush of poly(2-vinylpyridine) (P2VP, a weak cationic polyelectrolyte) demonstrated a pronounced shift in the position of the LSPR extinction band by 50 nm by varying the solution's pH within a relatively narrow range near the coil-to-globule transition of P2VP chains (the apparent pK_a ~3.8).[28] On the downside, the rather acidic range of pH values that can be measured with this device makes it of limited value for bioanalytical applications. The aforementioned drawback was partially addressed in the system composed of a hydrogel thin film of an ionically cross-linked alginate-gelatin complex.[30] The films showed the volume phase transition in the pH region near the pK_a value of alginate (~4.5).

Poly(*N*,*N*′-dimethylaminoethyl methacrylate) (PDMAEMA) (M_w = 90.2 kg/mol, M_w/M_n 1.09, Polymer Source, Inc., Canada) has been selected for the present study because its apparent pK_a value is very close to the neutral pH (the reported pK_a values are within the range of 6.2 to 7.5).[31−33] A plasmonic device (Figure 1) was assembled on a glass slide substrate coated with gold nanoislands and modified with an anchoring layer of chemically cross-linked poly(glycidyl methacrylate) (PGMA).

Received: December 19, 2010
Accepted: January 24, 2011
Published: January 28, 2011

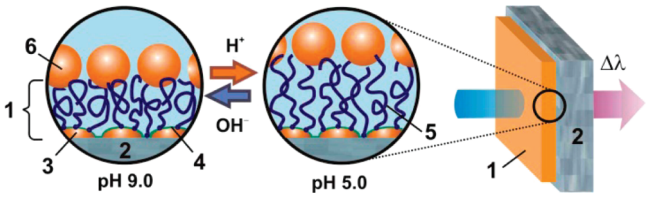

Figure 1. Plasmonic sensing platform consists of a responsive composite ultrathin film (1) prepared on a transparent glass substrate (2). The film is assembled from the following ingredients: gold nanoislands (3) immobilized on the glass substrate, an ~2 nm anchoring PGMA layer (4) deposited on the gold nanoislands, an ~7.6 nm PDMAEMA brush (5) "grafted to" the surface of the PGMA layer, and 12 nm colloidal gold nanoparticles (6) adsorbed on the brush surface.

The modification of the substrate has been described in detail elsewhere.[30] Briefly, gold nanoislands were evaporated on transparent glass slides (nominal thickness of the gold islands was 4 nm) and annealed overnight in a vacuum oven at 140 °C. A thin layer of PGMA (2.3 ± 0.5 nm thick) was deposited by spin-coating from a 0.01% solution in methylethylketone (MEK) and cross-linked overnight at room temperature to form a stable and strongly adhered anchoring layer.[34] Highly polished Si wafers modified with a PGMA anchoring layer were used as model substrates for ellipsometric measurements of the layer thickness.

A PDMAEMA brush was grafted onto the modified substrate in the next step. A thin film of PDMAEMA was deposited by spin-coating at 2000 rpm from a 0.15 wt % solution in MEK, annealed at 135 °C for 6 h in a vacuum oven (at ~1 Torr), and then washed three times in MEK and once in water for 10 min to remove the ungrafted polymer. PDMAEMA chains were grafted to the surface of the anchoring layer via the reaction of side tertiary amino groups of PDMAEMA and epoxy groups of PGMA occurring at the elevated temperature.[35] The resulting brush had a thickness of 7.6 ± 0.8 nm as determined independently by the scratch analysis (the brush was scratched by a sharp needle, and the scratch edge was scanned using atomic force microscopy (AFM) in order to determine the step height) and ellipsometry (PGMA-coated silicon wafers without gold nanoislands were used as model substrates in this case).

In the final step, 11.7 ± 0.9 nm citrate capped gold nanoparticles were adsorbed onto the PDMAEMA brush from an aqueous dispersion for 4 h. The synthesis of the gold nanoparticles is described elsewhere.[36]

A series of UV−vis spectra of the PDMAEMA-brush plasmonic platform in an unbuffered aqueous medium was obtained by titration with a base from pH 4 to pH 9. The individual spectra presented in Figure 2A exhibit a distinct extinction band that is, in fact, the superposition of the characteristic LSPR peaks of the gold nanoparticles and nanoislands. The position of the extinction band maximum showed a pronounced red shift with increase in the solution pH. The magnitude of the shift was comparable to the values reported in the literature for other platforms relying on the polymer-mediated plasmon coupling.[10,13,14,23] In Figure 2B, we plotted the shift in the band position ($\Delta\lambda_{max}$) versus the solution pH. The experimental points (black squares) were fitted with a sigmoid curve (solid line) that had the inflection point at pH 7.0; this value can be attributed to the apparent pK_a value of PDMAEMA. It is important to emphasize that no spectral shift was observed in the case when no gold nanoparticles were present on the brush surface; this result implies that the plasmon coupling between the particles and islands plays an important role.

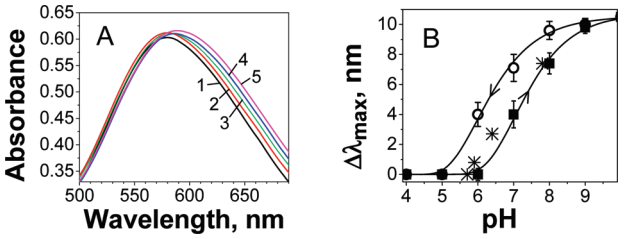

Figure 2. (A) Representative LSPR spectra of the plasmonic sensing device acquired in an unbuffered aqueous medium that was titrated with a base to the following pH values: 5 (1), 6 (2), 7 (3), 8 (4), and 9 (5). Shifts in $\Delta\lambda_{max}$ as a function of the solution pH calculated on the basis of the experimental spectral data. The spectra were acquired in an unbuffered aqueous media that were titrated with base (black squares) and acid (hollow circles). The asterisks show $\Delta\lambda_{max}$-values acquired for the sensor immersed successively in 0.1 M phosphate buffers with the pH values: 5.7, 5.9, 6.4, and 7.8.

The obtained results can be rationalized as follows. PDMAEMA is a weak polycation with tertiary amine pendant groups. At pH < 6 (i.e., below the pK_a where the amino groups are protonated), the PDMAEMA brush is highly swollen due to the osmotic effect of counterions entrapped in the brush. At this swelling degree, the Au nanoparticles and the nanoislands appear to be effectively decoupled as concluded from the fact that the LSPR band position is insensitive to the solution's pH. A rise in the solution's pH leads to the deprotonation of the amino groups and the gradual shrinking of the brush. The shrinking, in turn, results in a decrease in the effective distance between the Au nanoparticles and the nanoislands to the point where plasmon modes of the Au nanoparticles and the nanoislands begin to overlap. The transition region observed on the $\Delta\lambda_{max}$ curve between pH 6 and pH 9 indicates an increase in the strength of the interparticle plasmon coupling upon the brush's shrinking. The brush ceases shrinking when nearly all amino groups are deprotonated. This state is reached at pH > 9, where no further shift in the LSPR band position is observed (see Figure 2B). The proposed mechanism is in accordance with the previously reported systems based on gold nanoparticles and nanoislands.[26,28,29]

We carried out in situ ellipsometric measurements under water to measure the degree of swelling of the PDMAEMA brush in the protonated (pH 4) and deprotonated (pH 9) states. The measured values were 3.3 and 2.3, respectively, which are comparable to the results obtained by Tran and et al. who studied the swelling of PDMAEMA brushes prepared by the "grafting from" method with ellipsometry and neutron reflectivity.[37] The same group reported that the deprotonated PDMAEMA brush behaved as a neutral brush in a good solvent. The hydrophilic nature of deprotonated PDMAEMA has been also demonstrated in the studies of the phase behavior of the polymer in aqueous solutions.[27] The fact that the PDMAEMA brush remains largely swollen at basic pH values explains the smaller spectral sensitivity of the present plasmonic device compared with the P2VP-brush-based system.

We found that at the ionic strength of 0.1 M (representing the physiological level) the $\Delta\lambda_{max}$ curve shifted toward the lower pH values (the experimental data are shown with asterisks in Figure 2B). This result is rationalized by the fact that an increase in the ionic strength and the associated electrostatic screening of the charges along the polymeric chains caused the chains to adopt a more compact conformation. Such a conformational change, in turn, translated into the stronger interparticle plasmon

coupling at a given pH value compared with the solutions at low ionic strength.

An interesting finding was that the response of the plasmonic sensing device depended on the titration direction. In particular, Figure 2B shows that there is a pronounced shift between the $\Delta\lambda_{max}$-curves obtained in the cases when the solution pH was varied from pH 4 to pH 9 and when the pH decreased from pH 9 to pH 4 (the measurements were carried out in the solutions with no added salt). This behavior is a manifestation of the swelling hysteresis; it has been observed in many polyelectrolyte materials and usually originates from the hydrophobic interactions of aliphatic backbones as well as nonpolar moieties in pendant groups of some polyelectrolytes.[6] Such interactions hinder the protonation of amino groups of PDMAEMA chains. Thus, the swelling transition of the PDMAEMA brush shifts toward the lower pH values. The spectral shifts were completely reversible, as confirmed by repeating the titration procedure four times. This result implies that the plasmonic device is stable and can be used multiple times without significant deterioration in the optical response.

In our previous study, we demonstrated a biochemical-to-optical signal transduction scheme based on the combination of the plasmonic device from the pH-sensitive alginate-gelatin hydrogel with silver nanoparticles and a biocatalytic reaction of glucose oxidase (GOx) with glucose.[30] Because this enzymatic process yielded gluconic acid, the reaction medium became more acidic. The changes in the solution pH were detected with the plasmonic device. Because this plasmonic device was sensitive only to pH values below 5, the enzymatic process had to produce a sufficient amount of gluconic acid to lower the initially neutral solution pH (such as in blood) to the detectable levels. In contrast to our previous work, the present system shows the optical response in a pH range from pH 5 to pH 9 (Figure 2B), i.e., below and above physiological pH 7.4. Thus, the PDMAEMA-based plasmonic platform is more versatile in terms of potential analytes.

To demonstrate the feasibility of the PDMAEMA-based plasmonic device for enzymatic sensors, we conducted the following experiment. The device was immersed in a cuvette with a 10 mM glucose aqueous solution (the concentration found in blood) at pH 7. Afterward, GOx (United States Biochemical Co.) was injected into the cuvette; the enzyme concentration was a variable. We followed a fixed-time procedure in which visual spectra were acquired at a certain period of time after the addition of the enzyme in the solution. The reaction of GOx with glucose proceeds in two stages: (1) GOx catalyzes the oxidation of glucose to gluconolactone and hydrogen peroxide, using molecular oxygen as the electron acceptor, and (2) gluconolactone hydrolyzes spontaneously to gluconic acid. The hydrolysis reaction is a time-limiting stage, and its half-time at room temperature at pH 7 is ca. 10 min.[38] The response of the plasmonic device as measured 10 min after the injection of GOx into the cuvette was found to depend on the amount of the enzyme added to the solution. In Figure 3A, $\Delta\lambda_{max}$ values are plotted as a function of the enzyme concentration. Alternatively, changes in the absorbance determined at the fixed wavelength can be used as a measured parameter (Figure 3B). The chosen wavelength of 633 nm is accessible with commercial He−Ne lasers and solid-state laser diodes. The plots show that for the specified glucose concentration and reaction time at least 40 units of GOx are required to approach the maximum spectral shift by 10 nm.

In summary, we developed a plasmonic sensing platform that enables the transduction of changes in the solution pH into a pronounced optical signal in the visible spectral range. The platform is based on ultrathin pH-responsive polymer brush/gold nanoparticle composite films. The main advantage of the present system is that the solution pH can be measured within near-physiological range (between pH 5 and pH 9) which opens possibilities for the coupling to many enzymatic reactions that yield or consume protons.

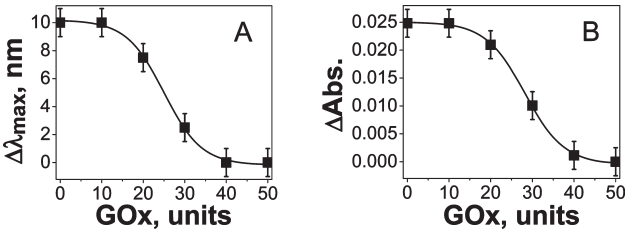

Figure 3. (A) Shifts in λ_{max} and (B) changes in the absorbance at λ = 633 nm as functions of the GOx concentration for the plasmonic sensing device in aqueous solutions containing 10 mM glucose. The spectral data were collected after the incubation period of 10 min.

AUTHOR INFORMATION

Corresponding Author
*E-mail: sminko@clarkson.edu.

ACKNOWLEDGMENT

The authors gratefully acknowledge the support of the U.S. Army via Grant W911NF-05-1-0339

REFERENCES

(1) Stewart, M. E.; Anderton, C. R.; Thompson, L. B.; Maria, J.; Gray, S. K.; Rogers, J. A.; Nuzzo, R. G. *Chem. Rev.* **2008**, *108*, 494–521.
(2) Ofir, Y.; Samanta, B.; Rotello, V. M. *Chem. Soc. Rev.* **2008**, *37*, 1814–1823.
(3) Wilson, R. *Chem. Soc. Rev.* **2008**, *37*, 2028–2045.
(4) Haes, A. J.; Van Duyne, R. P. *Anal. Bioanal. Chem.* **2004**, *379*, 920–930.
(5) Willets, K. A.; Van Duyne, R. P. *Annu. Rev. Phys. Chem.* **2007**, *58*, 267–297.
(6) Tokarev, I.; Minko, S. *Soft Matter* **2009**, *5*, 511–524.
(7) Tokarev, I.; Motornov, M.; Minko, S. *J. Mater. Chem.* **2009**, *19*, 6932–6948.
(8) Luzinov, I.; Minko, S.; Tsukruk, V. V. *Soft Matter* **2008**, *4*, 714–725.
(9) Azzaroni, O.; Brown, A. A.; Cheng, N.; Wei, A.; Jonas, A. M.; Huck, W. T. S. *J. Mater. Chem.* **2007**, *17*, 3433–3439.
(10) Gupta, S.; Agrawal, M.; Uhlmann, P.; Simon, F.; Oertel, U.; Stamm, M. *Macromolecules* **2008**, *41*, 8152–8158.
(11) Gupta, S.; Uhlmann, P.; Agrawal, M.; Chapuis, S.; Oertel, U.; Stamm, M. *Macromolecules* **2008**, *41*, 2874–2879.
(12) Mitsuishi, M.; Koishikawa, Y.; Tanaka, H.; Sato, E.; Makayama, T.; Matsui, J.; Miyashita, T. *Langmuir* **2007**, *23*, 7472–7474.
(13) Lee, S.; Perez-Luna, V. H. *Langmuir* **2007**, *23*, 5097–5099.
(14) Gupta, S.; Agrawal, M.; Uhlmann, P.; Simon, F.; Stamm, M. *Chem. Mater.* **2010**, *22*, 504–509.
(15) Diamanti, S.; Arifuzzaman, S.; Genzer, J.; Vaia, R. A. *ACS Nano* **2009**, *3*, 807–818.
(16) Li, D. X.; He, Q. A.; Li, J. B. *Adv. Colloid Interface Sci.* **2009**, *149*, 28–38.
(17) Lupitskyy, R.; Motornov, M.; Minko, S. *Langmuir* **2008**, *24*, 8976–8980.
(18) Li, D. X.; He, Q.; Cui, Y.; Li, J. B. *Chem. Mater.* **2007**, *19*, 412–417.

(19) Chakraborty, S.; Bishnoi, S. W.; Perez-Luna, V. H. *J. Phys. Chem. C* **2010**, *114*, 5947–5955.
(20) Liu, X. Y.; Cheng, F.; Liu, Y.; Li, W. G.; Chen, Y.; Pan, H.; Liu, H. J. *J. Mater. Chem.* **2010**, *20*, 278–284.
(21) Karg, M.; Hellweg, T. *Mater. Chem.* **2009**, *19*, 8714–8727.
(22) Jiang, G. Q.; Baba, A.; Ikarashi, H.; Xu, R. S.; Locklin, J.; Kashif, K. R.; Shinbo, K.; Kato, K.; Kaneko, F.; Advincula, R. *J. Phys. Chem. C* **2007**, *111*, 18687–18694.
(23) Kozlovskaya, V.; Kharlampieva, E.; Khanal, B. P.; Manna, P.; Zubarev, E. R.; Tsukruk, V. V. *Chem. Mater.* **2008**, *20*, 7474–7485.
(24) Qi, Z. M.; Wei, M.; Honma, I.; Zhou, H. *Chemphyschem* **2007**, *8*, 264–269.
(25) Karakouz, T.; Vaskevich, A.; Rubinstein, I. *J. Phys. Chem. B* **2008**, *112*, 14530–14538.
(26) Tokarev, I.; Tokareva, I.; Minko, S. *Adv. Mater.* **2008**, *20*, 2730–2734.
(27) Chang, S.; Singamaneni, S.; Kharlampieva, E.; Young, S. L.; Tsukruk, V. V. *Macromolecules* **2009**, *42*, 5781–5785.
(28) Tokareva, I.; Minko, S.; Fendler, J. H.; Hutter, E. *J. Am. Chem. Soc.* **2004**, *126*, 15950–15951.
(29) Tokareva, I.; Tokarev, I.; Minko, S.; Hutter, E.; Fendler, J. H. *Chem. Commun.* **2006**, *31*, 3343–3345.
(30) Tokarev, I.; Tokareva, I.; Gopishetty, V.; Katz, E.; Minko, S. *Adv. Mater.* **2010**, *22*, 1412–1416.
(31) van de Wetering, P.; Moret, E. E.; Schuurmans-Nieuwenbroek, N. M. E.; van Steenbergen, M. J.; Hennink, W. E. *Bioconjugate Chem.* **1999**, *10*, 589–597.
(32) Lee, A. S.; Gast, A. P.; Butun, V.; Armes, S. P. *Macromolecules* **1999**, *32*, 4302–4310.
(33) Plamper, F. A.; Ruppel, M.; Schmalz, A.; Borisov, O.; Ballauff, M.; Muller, A. H. E. *Macromolecules* **2007**, *40*, 8361–8366.
(34) Iyer, K. S.; Zdyrko, B.; Malz, H.; Pionteck, J.; Luzinov, I. *Macromolecules* **2003**, *36*, 6519–6526.
(35) Rocks, J.; Rintoul, L.; Vohwinkel, F.; George, G. *Polymer* **2004**, *45*, 6799–6811.
(36) Hutter, E.; Fendler, J. H.; Roy, D. *J. Phys. Chem. B* **2001**, *105*, 11159–11168.
(37) Sanjuan, S.; Perrin, P.; Pantoustier, N.; Tran, Y. *Langmuir* **2007**, *23*, 5769–5778.
(38) Pocker, Y.; Green, E. *J. Am. Chem. Soc.* **1973**, *95*, 113–119.